OUKA
The University of Osaka
Institutional Knowledge Archive

Title	Elastic constants of beta tungsten thin films studied by picosecond ultrasonics and density functional theory
Author(s)	Nagakubo, A.; Lee, H. T.; Ogi, H. et al.
Citation	Applied Physics Letters. 2020, 116(2), p. 021901-1-021901-5
Version Type	VoR
URL	https://hdl.handle.net/11094/83934
rights	Copyright 2020 Author(s). This article may be downloaded for personal use only. Any other use requires prior permission of the author and AIP Publishing. This article appeared in Applied Physics Letters, 116(2), 021901, 2020 and may be found at https://doi.org/10.1063/1.5131768.
Note	

The University of Osaka Institutional Knowledge Archive : OUKA

https://ir.library.osaka-u.ac.jp/

The University of Osaka

Applied Physics Letters

Elastic constants of beta tungsten thin films studied by picosecond ultrasonics and density functional theory

Cite as: Appl. Phys. Lett. **116**, 021901 (2020); https://doi.org/10.1063/1.5131768
Submitted: 15 October 2019 . Accepted: 26 December 2019 . Published Online: 13 January 2020

A. Nagakubo, H. T. Lee, H. Ogi, T. Moriyama, and T. Ono

View Online Export Citation CrossMark

© 2020 Author(s).

AIP Publishing

Applied Physics Letters ARTICLE scitation.org/journal/apl

Elastic constants of beta tungsten thin films studied by picosecond ultrasonics and density functional theory

Cite as: Appl. Phys. Lett. **116**, 021901 (2020); doi: 10.1063/1.5131768
Submitted: 15 October 2019 · Accepted: 26 December 2019 ·
Published Online: 13 January 2020

View Online Export Citation CrossMark

A. Nagakubo,[1,a)] H. T. Lee,[1] H. Ogi,[1] T. Moriyama,[2] and T. Ono[2]

AFFILIATIONS

[1]Graduate School of Engineering, Osaka University, Suita, Osaka 565-0871, Japan
[2]Institute for Chemical Research, Kyoto University, Uji, Kyoto 611-0011, Japan

[a)]nagakubo@prec.eng.osaka-u.ac.jp

ABSTRACT

Tungsten thin films are used for various applications and sometimes exhibit an A15 structure (β-W). They have some superior properties in comparison to the bcc structure (α-W), such as a higher superconducting transition temperature and larger spin Hall angle. However, elastic constants of β-W are unclear, which restricts mechanical applications and reliable density-functional-theory calculations. In this study, we synthesized α-W, β-W, and mixed-phase W films and determined their elastic constants by picosecond ultrasonics. We also calculated the elastic constants based on density functional theory and reveal that β-W has a larger elastic anisotropy and smaller shear modulus. Our calculation further indicates a stable stacking faulted β-W, which leads to a monoclinic structure.

Published under license by AIP Publishing. https://doi.org/10.1063/1.5131768

Tungsten is an important material because of its large mass density, high melting point, high heat resistance, and high mechanical strength. For example, hardness of tungsten carbide exceeds 20 GPa,[1,2] allowing the application as plasma facing materials in nuclear fusion devices to protect the vessel wall from intense particles and heat fluxes.[3–5] Tungsten thin films are also important functional materials with wide applications in mechanical coating layers,[6,7] acoustic multilayer reflectors,[8,9] X-ray mirrors,[10–12] or as spin current generators.[13] In these thin films, the structure and mechanical properties are important; however, they largely change depending on synthesis conditions. Tungsten shows a body-centered-cubic structure (α-W) at ordinary temperatures and pressures, but there also exists a metastable A15 structure (β-W),[14–16] and thin films sometimes show such a β-W structure, where oxygen plays an important role in stabilizing it.[17–22] (Note that β-W is not a suboxide such as W_3O[14] but a metallic phase.)[16,22,23]

β-W thin films show remarkable properties in comparison to α-W. The resistivity and superconducting transition temperature[24,25] are higher in β-W. Recently, large spin Hall angles[26–29] and hardness[7] have been reported in β-W, making it an attractive functional material. However, elastic constants—which are the most essential mechanical property—of β-W remain unclear. Slim *et al.* extracted monocrystal elastic constants of β-W from 2.1-μm α- and β-W films;[30] however, elastic constants of single-phase β-W have not been measured. Elastic constants reflect the intrinsic bond strength between atoms and correspond to the curvature of the interatomic potential. Therefore, they are related to strength,[31] hardness,[32,33] melting point,[34] and many thermodynamic properties. Furthermore, thin films often contain large residual stresses and many defects, and elastic constants are sensitive to them. An understanding of the mechanical properties of β-W thin films, and their dependence on defects and synthesis conditions, is of critical importance.

In this study, we measure the elastic constants of β-W and α-W thin films and their dependence on synthesis conditions using picosecond ultrasonics. We further calculate the elastic constants based on the density functional theory (DFT) and compare them with the experimental results to validate the calculation conditions. Finding good agreement, we theoretically study the impact of stacking faults on the stability of β-W and its effect on elastic constants to gain insight into how defects affect the structure of β-W thin films.

Synthesis conditions are important to make pure α-W and β-W thin films. For example, the surface oxide layer on a sputtering target is an important factor in forming β-W.[35] Base pressure hardly affects the phases between 2.7×10^{-7} and 6.7×10^{-5} Pa,[18] whereas Ar pressure during sputtering[21,22,36–39] and mixing gas of O_2[23] or N_2[40] largely affects the phases. The most important mechanism to form β-W is the

Published under license by AIP Publishing

phase transition from β-W to α-W. It has been reported that tungsten thin film has a critical thickness, above which β-W transforms into α-W,[17,20,37,41,42] and the phase-transition mechanism was attributed to an increase in temperature ($\sim$400 K) during deposition.[19,20] However, a postannealing procedure at about 900 K is needed for the phase transition,[21–23] and substrate heating during deposition did not cause the phase transition until 600 K.[43] Therefore, elevated temperature will not be the critical cause for the phase transition. Choi proposed that kinetic energy of tungsten and argon during sputtering drives atomic diffusion and the phase transition.[43] This mechanism can be applied to the phase-transition dependence on Ar pressure, sputtering power,[20,36] and bias voltage on the substrate:[36] low Ar pressure contributes to the phase transition because the mean free path and kinetic energy increase as the pressure decreases.[36] Higher sputtering power and negative bias voltage on the substrate also enhance the kinetic energy and atomic diffusion, which results in the phase transition.

Therefore, we synthesized β-W, α-W, and mixed-phase W (mix-W) thin films by the DC sputtering method by changing the sputtering pressure and power. Pure α-W and mix-W films were obtained by changing Ar pressure P_{Ar} between 0.2 and 0.6 Pa. The base pressure P_b and sputtering power were 8.77–13.4 $\times$ 10^{-6} Pa and $\sim$150 W, respectively. On the other hand, we synthesized pure β-W with P_b and P_{Ar} of 1.3 $\times$ 10^{-4} and 0.27 Pa, respectively. We reduced the sputtering power and presputtering time to be 60 W and a few minutes to obtain β-W. All of the films were deposited on Si (111) substrates, and the film thickness was about 40 or 70 nm. Note that we obtained almost the same structure among 40-nm and 70-nm films (Fig. S1 in the supplementary material).

We identified the tungsten structure by the X-ray diffraction (XRD) method using a Co target. We obtained pure α-W films at P_{Ar} = 0.21 Pa as seen from the measured spectra [Fig. S1(a)]. All of the diffraction peaks from α-W appear, and the other peaks come from the Si substrate. (The diffraction peak of α-W (200) appears around 69.2°; however, it is so close to the strong Si-substrate peak that we cannot distinguish them.) From the observed peaks, we determined the lattice constant a to be 3.1728 $\pm$ 0.0023 Å, which agrees well with the reported bulk value within 0.2%.[44]

As the Ar pressure increases, the lattice constant of α-W decreases, and β-W appears at P_{Ar} = 0.6 Pa. The Ar pressure dependence is consistent with previous studies.[22,37,39] However, the α-W phase coexists even at P_{Ar} = 0.6 Pa, and good single-phase β-W cannot be obtained by only increasing the Ar pressure because it deteriorates the film structure. We measured the film thickness d, mass density ρ, and surface roughness by the X-ray reflection (XRR) method.[45] As the Ar pressure increases, the critical angle becomes small and the attenuation of the periodic reflectivity change becomes large [Fig. S1(b)], which corresponds to a decrease in mass density and an increase in roughness, respectively. The Ar pressure dependence of mass density and roughness is shown in Fig. 1(a). The Ar pressure largely affects not only the crystal phases but also the roughness and mass density; as Ar pressure increases, mass density decreases in spite of a decrease in the lattice constant, which indicates that the films include many voids and mechanical properties will be significantly deteriorated.

To evaluate the mechanical property change of the films, we measured the longitudinal-wave elastic constants C_L by picosecond ultrasonics.[46,47] We used a titanium sapphire pulse laser, whose wavelength

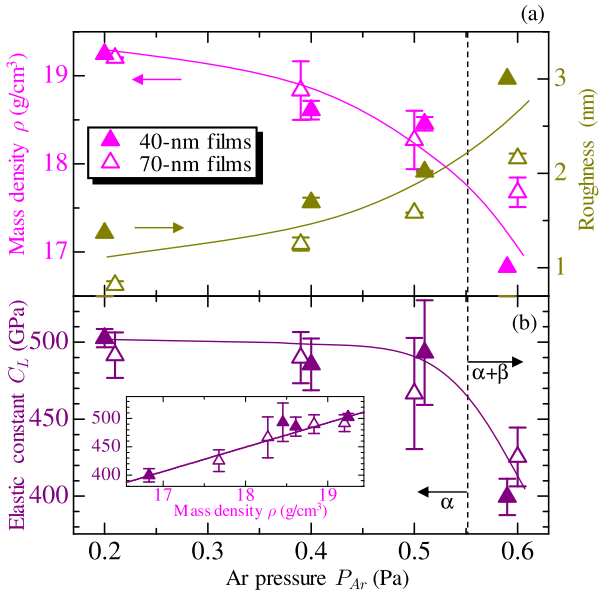

FIG. 1. Dependence of (a) mass density ρ or roughness, and (b) the elastic constant C_L of mix-phase W film specimens on Ar pressure. The inset figure in (b) shows the relationship between ρ and C_L.

and repetition rate are 800 nm and 80 MHz, respectively. We controlled the light path of the pump light by corner reflectors and a stage controller and modulated the pump light pulses as 100 kHz. The wavelength of the probe light was converted into 400 nm. Both light normally entered a specimen through an objective lens.[48] The pump light pulse excites a strain pulse at the film surface, which leads to through-thickness resonances or pulse-echo signals for the 40-nm or 70-nm films, respectively (in Fig. S2). Because the acoustic impedance of tungsten is larger than that of Si, the frequency f_n of the nth-order through-thickness resonance is given by $f_n = nv_L/2d$, where $v_L = \sqrt{C_L/\rho}$ is the longitudinal-wave sound velocity.[49] The period τ of the pulse echoes corresponds to the round trip time of the strain pulse, which is given by $\tau = 2d/v_L$.[50]

C_L of the films significantly decreases as the Ar pressure increases as shown in Fig. 1(b). In particular, C_L of the mix-W film (P_{Ar} = 0.6 Pa) is smaller than that of the pure α-W film (P_{Ar} = 0.2 Pa) by 17%. This decrease is caused by defects: the measured mass density ρ of the mix-W films is smaller than the theoretical mass density by 8%, and their surface roughness is large (about 5% of the thickness). Therefore, the defects deteriorate the mechanical properties of the mix-W films. We find that the structural changes due to Ar pressure significantly affect the elastic constant, and the decrease in the elastic constant is related to the decrease in mass density ρ as shown in the inset of Fig. 1(b).

We synthesized pure β-W films by the low-power and low-base-pressure conditions. The measured XRD spectrum is shown in Fig. S1(a) (blue). From the measured diffraction angles, we determined the lattice constant of the β-W film as 5.0543 $\pm$ 0.0010 Å. We also confirmed that the β-W film comprises the metallic tungsten phase by X-ray photoelectron spectroscopy (XPS): at the surface, we observed four XPS peaks between 30 and 40 eV [in Fig. S3(a)], which correspond to 4f peaks of W and WO_3.[21] We also observed the O(1s) and

Published under license by AIP Publishing

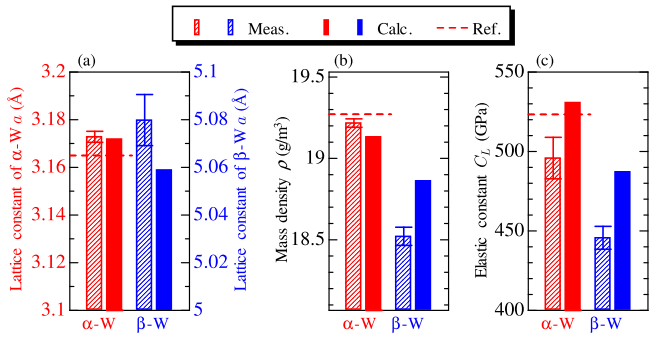

FIG. 2. Measured (hatched bars), calculated (solid bars), and reported values (dashed lines)[14,16,44,51] of (a) lattice constant *a*, (b) mass density ρ, and (c) the elastic constant C_L of pure α-W and β-W.

C(1*s*) peaks at around 532 and 285 eV, respectively. However, the O, C, and WO_3 peaks disappeared following a few minutes sputtering in the XPS chamber, and only the metallic-bond peaks [W($4f_{7/2}$), W($4f_{5/2}$), and W($5p_{3/2}$)] remain. Furthermore, the Rutherford backscattering spectrometry (RBS) spectrum is shown in Fig. S3(d). The observed spectra agree well with the simulation result for the tungsten film on the Si substrate, using the ρ and *d* parameters for the film determined from the XRR measurement. We could not fit the experimental results by assuming WO_3. These results strongly support that the synthesized β-W film mainly consists of the metallic tungsten phase excluding the surface oxide layer. Previous β-W films also exhibit surface oxide layers,[17,21–23,35] which are formed by air exposure.[22]

The measured elastic constants C_L of pure α-W and β-W are 496 ± 13 and 446 ± 7 GPa, respectively. C_L of the pure α-W film is lower than the corresponding bulk value[51] by 5.4% similar to the usual metallic thin films (thin films often show 5–20% lower elastic constants than bulks due to defects).[49,52–54] We find that C_L of β-W is lower than that of the pure α-W film by 10%. Elastic constants of bulk β-W have not been reported since pure bulk β-W was not obtained. Previous bulk specimens have a small mass density of 15.0 g/cm^3 and are considered to be W_3O.[14] From mix-W films, Slim *et al.* determined C_{11} of monocrystal β-W to be 350.3 ± 45.6 GPa.[30] We attribute these discrepancies to the specimen difference: we used 40-nm and 70-nm pure β-W films; on the other hand, Slim *et al.* used 2–3 μm mix-W films.

To calculate the elastic constants of β-W and discuss its stability, we performed the DFT calculation using the Vienna *ab initio* simulation package (VASP)[55] with projector augmented wave potentials[56,57] and the generalized gradient approximation (GGA) proposed by Perdew *et al.*[58] We also applied local density approximation (LDA),[59,60] which failed to give good agreement with our experimental values in this work. We evaluated the dependence of the lattice constant and elastic constants on the cutoff energy of the plane wave and used enough high cutoff energy. The cutoff energy and the *k*-point mesh were 1560 eV and 14 × 14 × 14 for α-W and 1300 eV and 16 × 16 × 16 for β-W, respectively. We consider six valence electrons for each W atom.

The calculation results agree well with the experimental results in this study and previous reports. The differences in the lattice constant, the mass density, and the elastic constant of α-W among the calculated, measured, and reported values are 0.2%, 0.7%, and 7%, respectively, as shown in Fig. 2 and Table I. For β-W, the measured and calculated lattice constants agree with each other within 0.4%, while the reported lattice constant is 0.8% lower than our measurement value. The differences between the measured and calculated values in ρ and C_L are 1.9% and 8%, respectively, which agree well with each other in spite of the difficulties in determining the elastic constants in thin film and DFT calculation. Our calculation indicates that β-W exhibits larger elastic anisotropy than α-W; C_{11} of β-W is larger than that of α-W, while C_{44} of β-W is smaller than that of α-W, resulting in the universal anisotropy index[61] A^U of 0.028 and 0.79 for α-W and

TABLE I. Determined and reported mass density ρ, lattice constant *a*, longitudinal-wave velocity v_L, the corresponding elastic constant C_L, and monocrystal elastic constants C_{11}, C_{12}, and C_{44} for each phase and Ar pressure P_{Ar}.

	Phase	P_{Ar} (Pa)	ρ (g/cm^3)	*a* (Å)	v_L (m/s)	C_L (GPa)	C_{11}	C_{12}	C_{44}
Measure	Pure α	0.20	19.22 ±0.03	3.1728 ±0.0023	5079 ±66	496 ±13			
	α	0.40	18.72 ± 0.24	3.1569 ± 0.0007	5105 ± 85	487 ± 16			
	α	0.50	18.36 ±0.22	3.1540 ±0.0013	5119 ±189	482 ±36			
	α and β	0.59	17.39 ±0.50	3.1583 ±0.0005	4890 ±91	414 ±21			
				5.0543 ±0.0010					
	Pure β	0.27	18.52 ±0.06	5.0798 ±0.0107	4907 ±39	446 ±7			
Calc.	Pure α		19.13	3.1719	5267	530.8	551.5	198.1	151.6
	Pure β		18.86	5.0589	5082	487.2	595.0	162.2	98.1
	S_1		19.13	5.0350[a]	5210	519.3	515.8[b]	214.0[b]	157.7[b]
Ref.	Pure α		19.27[c]	3.1652[e]	5216[c]	524.3[c]	523.3[c]	204.5[c]	160.7[c]
	β		19.12[d]	5.036[d]		393.9[f]	350.3[f]	108.8[f]	180.1[f]

[a]Cube root of the volume.
[b]Average values of the corresponding components.
[c]Reference 51.
[d]References 14 and 16.
[e]Reference 44.
[f]Reference 30.

Published under license by AIP Publishing

β-W, respectively. Slim *et al.* also reported that β-W has larger anisotropy.

Our calculation further indicates a stable stacking faulted β-W structure and elastic softening due to the stacking fault. β-W contains eight atoms in the unit cell within four layers as follows: A layer (0, 0, 0), $\left(\frac{1}{2},\frac{1}{4},0\right)$, $\left(\frac{1}{2},\frac{3}{4},0\right)$, B_1 layer $\left(0,\frac{1}{2},\frac{1}{4}\right)$, C layer $\left(\frac{1}{2},\frac{1}{2},\frac{1}{2}\right)$, $\left(\frac{3}{4},0,\frac{1}{2}\right)$, $\left(\frac{1}{4},0,\frac{1}{2}\right)$, and B_2 layer $\left(0,\frac{1}{2},\frac{3}{4}\right)$ as shown in Figs. 3(a) and 3(b). However, previous XRD[20] and energy-filtered electron diffraction[21–23] measurements indicate that β-W comprises the normal-ordered structure (ABCB stacking) and stacking faulted structure of ABAB stacking (S_1)[20–23] and AB'CB stacking (S_2).[20] We evaluate their crystal stability and stiffness using the same calculation condition as β-W and reveal that S_1-W and S_2-W are unstable for shear strain and transform into monoclinic structures. By the relaxation calculation from the initial S_1 and S_2 structures, we obtained the orthorhombic structure with keeping the initial stacking layers; however, their shear moduli are negative and S_1-W converges in the monoclinic structure as shown in Fig. 3(c). The total energies per unit volume of α-W, β-W, and S_1-W are -0.82, -0.80, and -0.78 eV/Å^3, respectively. On the other hand, S_2-W shows a completely different monoclinic structure, and its total energy per unit volume is -0.63 eV/Å^3, which is considerably higher and unstable. We consider that S_1-W can be easily formed under a residual stress in the film like in previous studies[20–23] because of the small energy difference while S_2-W would not be contained. The mechanical properties of S_1-W are close to those of α-W; the calculated ρ and C_L values of S_1-W are 19 133 kg/m^3 and 519.3 GPa, respectively, as shown in Table I (all independent components are listed in Table SI). These results indicate that stacking-faulted β-W intends to transform into S_1-W. However, the phase transition requires large shear deformation, and the initial stacking faulted structure is unstable. Our calculation indicates that the β-W film contains the stacking faulted structure, which decreases elastic constants.

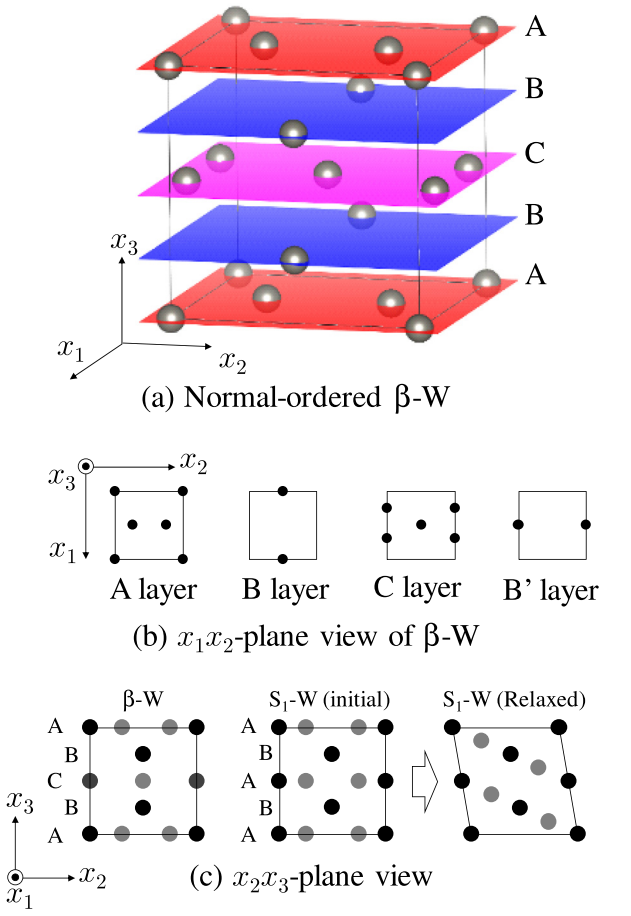

FIG. 3. (a) The structure of normal-ordered (ABCB-stacking) β-W. (b) The x_1x_2 plain view of A, B, C, and B' layers. (c) The x_2x_3 plain view of β-W, initial S_1-W, and relaxed S_1-W.

To conclude, we synthesized mixed-phase W films by increasing Ar pressure during sputtering and measured their mass density and the longitudinal-wave elastic constant. The increase in Ar pressure deteriorates the film structure and mechanical properties, which leads to a 17% decrease in the elastic constant. We also synthesized pure α-W and β-W and determined the lattice constant, mass density, and elastic constants of β-W. The isotropic longitudinal elastic constant of β-W is smaller than that of α-W. Based on the DFT calculation, we find that the shear modulus of β-W is 35% smaller than that of α-W. Our calculation further indicates that stacking faulted β-W takes a stable structure, whose mechanical properties are identical to α-W.

See the supplementary material for the details of the XRD and XRR spectra (Fig. S1), waveforms and extracted signals (Fig. S2), XPS and RBS spectra (Fig. S3), and calculated lattice constants and elastic constants for α-W, β-W, S_1-W, and S_2-W (Table SI).

We really acknowledge Professor Kusakabe, Osaka University, for important and helpful discussion about the density-functional-theory calculation. This work was supported by JSPS KAKENHI Grant No. JP17JD7186 (Grant-in-Aid for JSPS Fellows).

REFERENCES

[1]H. C. Lee and J. Gurland, Mater. Sci. Technol. **33**, 125 (1978).
[2]Z. Z. Fang, X. Wang, T. Ryu, K. S. Hwang, and H. Y. Sohn, Int. J. Refract. Met. Hard Mater. **27**, 288 (2009).
[3]M. Rieth, S. L. Dudarev, S. M. Gonzalez de Vicente, J. Aktaa, T. Ahlgren, S. Antusch, D. E. J. Armstrong, M. Balden, N. Baluc, M. F. Barthe *et al.*, J. Nucl. Mater. **442**, S173 (2013).
[4]S. J. Zinkle, J. P. Blanchard, R. W. Callis, C. E. Kessel, R. J. Kurtz, P. J. Lee, K. A. McCarthy, N. B. Morley, F. Najmabadi, R. E. Nygren, G. R. Tynan, D. G. Whyte, R. S. Willms, and B. D. Wirth, J. Nucl. Mater. **89**, 1579 (2014).
[5]G. R. Tynan, R. P. Doerner, J. Barton, R. Chen, S. Cui, M. Simmonds, Y. Wang, J. S. Weauver, N. Mara, and S. Pathak, Nucl. Mater. Energy **12**, 164 (2017).
[6]L. C. A. Morimitsu, J. D. L. Roche, A. Ruden, D. Escobar, and E. R. Parra, Chem. Phys. Lett. **40**, 6383 (2014).
[7]H. L. Sun, Z. X. Song, D. G. Guo, F. Ma, and K. W. Xu, J. Mater. Sci. Technol. **26**, 87 (2010).
[8]M. Yim, D. H. Kim, D. Chai, and G. Yoon, J. Vac. Sci. Technol., A **22**, 465 (2004).
[9]S. Jose, A. B. M. Jansman, R. J. E. Hueting, and J. Schmitz, IEEE Trans. Ultrason. Ferroelectr. Freq. Control **57**, 2753 (2010).
[10]T. Salditt, D. Lott, T. H. Metzger, J. Peisl, G. Vignaud, P. Høghøj, O. Schärpf, P. Hinze, and R. Lauer, Phys. Rev. B **54**, 5860 (1996).
[11]M. H. Modi, G. S. Lodha, S. R. Naik, A. K. Srivastava, and R. V. Nandedkar, Thin Solid Films **503**, 115 (2006).

Published under license by AIP Publishing

[12]P. N. Rao, S. K. Rai, M. Nayak, and G. S. Lodha, Appl. Opt. **52**, 6126 (2013).
[13]C. F. Pai, M. H. Nguyen, C. Belvin, L. H. V. Leão, D. C. Ralph, and R. A. Buhrman, Appl. Phys. Lett. **104**, 082407 (2014).
[14]G. Hägg and N. Schönberg, Acta Crystallogr. **7**, 351 (1954).
[15]G. Mannella and J. O. Hougen, J. Phys. Chem. **60**, 1148 (1956).
[16]W. R. Morcom, W. L. Worrell, H. G. Sell, and H. I. Kaplan, Metall. Trans. **5**, 155 (1974).
[17]I. A. Weerasekera, S. I. Shah, D. V. Baxter, and K. M. Unruh, Appl. Phys. Lett. **64**, 3231 (1994).
[18]D. Choi, B. Wang, S. Chung, X. Liu, A. Darbal, A. Wise, N. T. Nuhfer, K. Barmak, A. P. Warren, K. R. Coffey, and M. F. Toney, J. Vac. Sci. Technol., A **29**, 051512 (2011).
[19]S. M. Rossnagel, I. C. Noyan, and C. Cabral, J. Vac. Sci. Technol., B **20**, 2047 (2002).
[20]P. Petroff, T. T. Sheng, A. K. Sinha, G. A. Rozgonyi, and F. B. Alexander, J. Appl. Phys. **44**, 2545 (1973).
[21]Y. G. Shen and Y. W. Mai, J. Mater. Sci. **36**, 93 (2001).
[22]Y. G. Shen, Y. W. Mai, C. Zhang, D. R. McKenzie, W. D. McFall, and E. McBride, J. Appl. Phys. **87**, 177 (2000).
[23]Y. G. Shen and Y. W. Mai, Mater. Sci. Eng. A **284**, 176 (2000).
[24]W. L. Bond, A. S. Cooper, K. Andres, G. W. Hull, T. H. Geballe, and B. T. Matthias, Phys. Rev. Lett. **15**, 260 (1965).
[25]S. Basavaiah and S. R. Pollack, J. Appl. Phys. **39**, 5548 (1968).
[26]C. F. Pai, L. Liu, Y. Li, H. W. Tseng, D. C. Ralph, and R. A. Buhrman, Appl. Phys. Lett. **101**, 122404 (2012).
[27]Q. Hao, W. Chen, and G. Xiao, Appl. Phys. Lett. **106**, 182403 (2015).
[28]Q. Hao and G. Xiao, Phys. Rev. Appl. **3**, 034009 (2015).
[29]K. U. Demasius, T. Phung, W. Zhang, B. P. Hughes, S. H. Yang, A. Kellock, W. Han, A. Pushp, and S. S. P. Parkin, Nat. Commun. **7**, 10644 (2016).
[30]M. F. Slim, A. Alhussein, E. Zgheib, and M. François, Acta Mater. **175**, 348 (2019).
[31]O. D. Sherby and P. M. Burke, Prog. Mater. Sci. **13**, 323 (1968).
[32]D. M. Teter, MRS Bull. **23**, 22 (1998).
[33]A. Nagakubo, H. Ogi, H. Sumiya, and M. Hirao, Appl. Phys. Lett. **105**, 081906 (2014).
[34]H. J. Frost and M. F. Ashby, *Deformation-Mechanism Maps: The Plasticity and Creep of Metals and Ceramics* (Pergamon Press, Oxford, 1982), p. 18.
[35]M. J. Okeefe, J. T. Grant, and J. S. Solomon, J. Electron. Mater. **24**, 961 (1995).
[36]F. T. N. Vüllers and R. Spolenak, Thin Solid Films **577**, 26 (2015).
[37]T. J. Vink, W. Walrave, J. L. C. Daams, A. G. Dirks, M. A. J. Somers, and K. J. A. van den Aker, J. Appl. Phys. **74**, 988 (1993).
[38]K. Salamon, O. Milat, N. Radić, P. Dubček, M. Jerčinović, and S. Bernstorff, J. Phys. D **46**, 095304 (2013).
[39]I. Djerdj, A. M. Tonejc, A. Tonejc, and N. Radić, Vacuum **80**, 151 (2005).
[40]J. Liu and K. Barmak, Acta Mater. **104**, 223 (2016).
[41]I. C. Noyan, T. M. Shaw, and C. C. Goldsmith, J. Appl. Phys. **82**, 4300 (1997).
[42]J. S. Lee, J. Cho, and C. Y. You, J. Vac. Sci. Technol., A **34**, 021502 (2016).
[43]D. Choi, Microelectron. Eng. **183**, 19 (2017).
[44]W. Parrish, Acta Crystallogr. **13**, 838–184 (1960).
[45]L. G. Parratt, Phys. Rev. **95**, 359 (1954).
[46]C. Thomsen, J. Strait, Z. Vardeny, H. J. Maris, J. Tauc, and J. J. Hauser, Phys. Rev. Lett. **53**, 989 (1984).
[47]C. Thomsen, H. T. Grahn, H. J. Maris, and J. Tauc, Phys. Rev. B **34**, 4129 (1986).
[48]A. Nagakubo, A. Yamamoto, K. Tanigaki, H. Ogi, N. Nakamura, and M. Hirao, Jpn. J. Appl. Phys., Part 1 **51**, 07GA09 (2012).
[49]H. Ogi, M. Fujii, N. Nakamura, T. Shagawa, and M. Hirao, Appl. Phys. Lett. **90**, 191906 (2007).
[50]H. Ogi, M. Fujii, N. Nakamura, T. Yasui, and M. Hirao, Phys. Rev. Lett. **98**, 195503 (2007).
[51]F. H. Featherston and J. R. Neighbour, Phys. Rev. **130**, 1324 (1963).
[52]N. Nakamura, H. Ogi, T. Shagawa, and M. Hirao, Appl. Phys. Lett. **92**, 141901 (2008).
[53]H. Ogi, A. Yamamoto, K. Kondou, K. Nakano, K. Morita, N. Nakamura, T. Ono, and M. Hirao, Phys. Rev. B **82**, 155436 (2010).
[54]N. Nakamura, Y. Nakamichi, H. Ogi, M. Hirao, and M. Nishiyama, Jpn. J. Appl. Phys., Part 1 **52**, 07HB05 (2013).
[55]G. Kresse and J. Hafner, Phys. Rev. B **47**, 558 (1993).
[56]P. E. Blöchl, Phys. Rev. B **50**, 17953 (1994).
[57]G. Kresse and D. Joubert, Phys. Rev. B **59**, 1758 (1999).
[58]J. P. Perdew, K. Burke, and M. Ernzerhof, Phys. Rev. Lett. **77**, 3865 (1996).
[59]J. P. Perdew and A. Zunger, Phys. Rev. B **23**, 5048 (1981).
[60]J. P. Perdew and Y. Wang, Phys. Rev. B **45**, 13244 (1992).
[61]S. I. Ranganathan and M. O. Starzewski, Phys. Rev. Lett. **101**, 055504 (2008).

Published under license by AIP Publishing